UDC 004.8; 004.93

EFFICIENT MODEL ALGORITHMS FOR PROCESSING AND RECOGNIZING MICROSCOPIC OBJECT OF ANEMIA DISEASE

[+] *Iskandarova S.N.*[1], *Tulaganova F.K.*[1]

[1] Tashkent University of Information Technologies named after Muhammad al-Khwarizmi, Tashkent, Uzbekistan

[+] sayyora5@mail.ru

Abstract. Iron deficiency anemia (IDA) is a prevalent global health issue, often diagnosed through peripheral blood smear (PBS) analysis, which relies on experienced specialists and expensive equipment, making it prone to human error. This study aimed to develop and compare deep learning-based object detection algorithms to automate IDA diagnosis using PBS images, addressing the limitations of traditional methods. A dataset of 386 PBS images was collected from Kasturba Medical College, comprising 249 IDA cases and 137 normal samples, with 2,550 hypochromic microcytes annotated. Images were preprocessed using the Reinhard stain normalization method to correct color and illumination variations, enhancing model performance. The study evaluated YOLO (v5, v7, v8), Faster RCNN, RetinaNet, and DDOD models. YOLOv7-tiny achieved 86.2% mAP@0.5, surpassing traditional methods (80-85% accuracy). However, the RetinaNet-DDOD model (ResNet-101 backbone) outperformed others, achieving 93.4% mAP@0.5 and 75.3% mAP@0.5:0.95. Through 5-fold cross-validation, DDOD reached 94.8% AP@0.5, exceeding RetinaNet by 5%, a result validated by statistical analysis (Paired t-test, p=0.004; Cohen's D=-3). The DDOD model effectively detected overlapping cells with 92% accuracy and reduced false positives to 3.5%, though it faced challenges from a small dataset and sensitivity to color variations. Future work will focus on expanding the dataset and detecting other anemia types. This study demonstrates the potential of automated systems to enhance IDA diagnosis accuracy, reduce hematologists' workload, and accelerate clinical workflows, providing a foundation for broader applications in anemia diagnostics.

Keywords: Iron deficiency anemia (IDA), Peripheral blood smear (PBS), Object Detection, Deep Learning, RetinaNet-DDOD, YOLO models, Reinhard normalization, Hypochromic microcytes, mAP@0.5 metric, Automated diagnosis.

1 INTRODUCTION

Anemia is a widespread global health issue, particularly posing serious health concerns among children and women. According to the World Health Organization (WHO), 40% of children aged 6–59 months, 37% of pregnant women, and 30% of women aged 15–49 suffer from anemia [1,11]. Iron deficiency anemia (IDA) is the most common type, and its initial diagnosis is typically carried out through microscopic analysis of peripheral blood smear (PBS) images [2-8]. Traditional methods require experienced hematologists and expensive laboratory equipment, which limits diagnostic capabilities in developing countries. Additionally, the possibility of human error can negatively affect diagnostic accuracy[9,10]. Therefore, automated systems—especially computer-aided diagnosis (CAD) systems—play a vital role in detecting anemia.Previous studies have mainly focused on traditional machine learning methods, often emphasizing segmentation and classification [12–19]. For example, Wong et al. achieved an F2-score of 94.8% using SVM and U-Net, while Purwar et al. reached 99% accuracy with AlexNet [20, 23]. However, these methods are time-consuming and involve complex segmentation processes. Today, deep learning technologies—particularly object detection algorithms—are recognized as effective solutions to these challenges. The aim of this paper is to propose an efficient object detection model, specifically the RetinaNet-DDOD algorithm, to detect hypochromic microcytes in PBS images and to compare its advantages over other models. The research is focused on automating IDA diagnosis to reduce the workload of hematologists and accelerate the diagnostic process[24, 30]. Previous studies on anemia detection have primarily relied on traditional machine learning and segmentation-based methods. Wong et al. [31, 33] achieved an F2-score of 94.8% in classifying abnormal red blood cells using SVM, TabNet, and U-Net; however, the issue of class imbalance remained unresolved. Parab et al. [34] classified RBC shapes using a 13-layer CNN and achieved 98.6% accuracy, but the segmentation process was complex Chandrasiri et

al [35, 36] demonstrated 91–97% accuracy in identifying elliptocytes, microcytes, and macrocytes, although the small dataset posed limitations. Pasupa et al [37] obtained a high F1-score using CNN-ResNet50 and DenseNet-121, but the class imbalance issue was not addressed. Azam et al [38,40] reached 96% accuracy using GLCM and Gabor features, but the limited number of images restricted the results. Rahman et al achieved 97% accuracy using the CAWPE method, although the color normalization process added additional complexity. Purwar et al combined AlexNet with clinical parameters to reach 99% accuracy, but the method was limited to distinguishing only two classes. The main limitations of these studies were the time-consuming nature of segmentation-based approaches and the challenges associated with working with small datasets. In contrast, object detection methods offer more efficient solutions by enabling faster and more flexible analysis through the use of bounding boxes [38, 40].

2 WORKS PERFORMED

In this study, 386 PBS (Peripheral Blood Smear) images were collected from Kasturba Medical College (KMC), comprising 249 cases of IDA (Iron Deficiency Anemia) and 137 normal samples. The images were captured at 100x magnification, with a resolution of 1216×912, and prepared using the Leishman staining technique. A total of 2,550 hypochromic microcytes were annotated, and the dataset was split into 70% training, 20% validation, and 10% testing sets.

For image preprocessing, the Reinhard stain normalization method was applied to correct color and illumination variations. The RGB images were converted into the LAB color space, and the L channel was normalized. The models used in the study included YOLO (v5, v7, v8), RetinaNet, and DDOD. Among these, the RetinaNet-DDOD model with ResNet-101 backbone achieved the best performance. Evaluation metrics included mAP@0.5 and mAP@0.5:0.95, which measured the accuracy and reliability of the models. The experiments were conducted on an HP EliteDesk 800 G4 system equipped with an NVIDIA GeForce RTX A6000 GPU.

2.1 Data Collection, Image Preprocessing, Models, and Evaluation Metrics

In this study, a total of 386 peripheral blood smear (PBS) images were collected from the Hematology Department of Kasturba Medical College (KMC). Among them, 249 were cases of iron deficiency anemia (IDA), while 137 were normal samples. The images were captured using an Olympus BX51 microscope with a DP80 camera at 100x magnification and a resolution of 1216×912 pixels. The samples were prepared using the Leishman staining technique. A total of 2,550 hypochromic microcytes were annotated using the LabelImg tool with bounding boxes. The dataset was divided into 70% training (337 images, 1848 objects), 20% validation (32 images, 480 objects), and 10% testing (17 images, 221 objects).

2.2 Image Preprocessing

To correct for color and illumination variations, the Reinhard stain normalization method was used during preprocessing. The RGB images were first converted to the LAB color space. Then, the L channel (lightness) was normalized, while the A and B channels (color information) were left unchanged to preserve chromatic content. After normalization, the L channel was recombined with the A and B channels, and the images were converted back to RGB format. This process ensured image consistency and improved model performance.

2.3 Models

The models used in this study included YOLO (v5, v7, v8), RetinaNet, and DDOD (Disentangled Dense Object Detector). YOLOv5 is based on the EfficientNet architecture and uses CIoU loss. YOLOv7-tiny incorporates E-ELAN blocks and re-parameterization techniques. YOLOv8 employs an anchor-free approach with C2f modules.

RetinaNet-DDOD demonstrated high effectiveness in detecting small and densely packed objects by leveraging focal loss and the Feature Pyramid Network (FPN). The DDOD model combined with a ResNet-101 backbone achieved the best results among the evaluated models.

The RetinaNet-DDOD architecture is designed for small and complex object detection. It works without segmentation, which speeds up analysis and increases its effectiveness in practical medical diagnostics (fig. 1).

1. The model is fed with a peripheral blood smear (PBS) image. This image may contain hypochromic microcytes. Images are typically captured at 1216×912 pixels and 100x magnification. 2. Backbone (ResNet-101). ResNet-101 is used as the main feature extraction part of the model. This deep convolutional neural network extracts useful visual features from the image. ResNet-101 has 101 layers, which helps to

train deep networks efficiently through skip-connections. 3. Feature Pyramid Network (FPN). FPN allows multi-dimensional feature detection by combining feature maps of different levels. This allows the model to detect small, medium, and large microcytes4. Classification Subnet. This subnet determines the object class (e.g., hypochromic microcyte or normal cell) for each bounding box. It performs the function of determining the category of objects in the image 5. Regression Subnet. This subnet determines the location and size of each object (bounding box coordinates). That is, it calculates the exact location of cells in the image 6. Focal LossThe Focal Loss function is used in the classification subnet. The advantage of this function is that it helps solve the problem of unbalanced classes. More attention is paid to rare classes (for example, microsites) 7. Smooth L1 Loss. The Smooth L1 Loss function is used for the regression subnet. This function serves to reduce the error in the bounding box coordinates, especially by smoothly penalizing small errors, making the model more stable 8. Output. The model output will consist of the following.

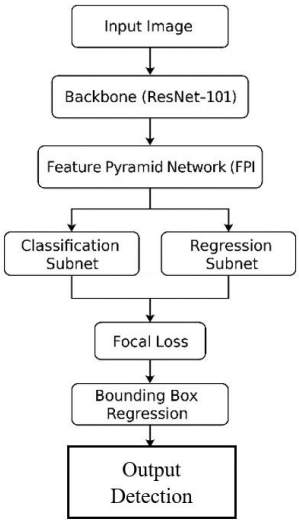

Fig. 1. Step-by-step architecture of the RetinaNet-DDOD (Disentangled Deense Object Detector) model

3 MATHEMATICAL MODEL

The input is a peripheral blood smear (PBS) image:

$$I \in \mathbb{R}^{H\times W\times 3}, \tag{1}$$

where $H = 912 W = 1216$, and 3 channels represent PGB.

This deep CNN extracts hierarchical features from the image. Each residual block user

$$x_{1+1} = f(x_l) + x_1, \tag{2}$$

where $f(x_l)$ – conwalution, batch norm, and ReLU, x_l – input to the residual black. Benefit: Skip connections enable deep training and help avoid vanishing gradients.

Combines features at different scales using a top-down architecture with lateral connections:

$$P_l = C_F + Upsample(P_{l+1}), \tag{3}$$

where C_F – feature from backbone at level l, P_l – pyramid output at level l. Upsample usually done by nearest-neighbor or bilinear interpolation.

For each anchor box, predicts the probobility p_i of object classes:

$$p_i = \sigma(z_i), \tag{4}$$

where z_i – raw scare (lagit) from the network, σ – sigmoid activation.

Designed to address class imbalance:

$$t_x = \frac{(x - x_a)}{w_e}, t_y = \frac{(y - \psi_a)}{h_a},$$
$$t_w = \log(\frac{w}{w_u}), t_k = \log(\frac{h}{h_e}), \tag{5}$$

where (x, y, w, h) – predicted box center and size, $(x_a, \forall_a, w_a, h_a)$ – anchar box center and size.

Designed to address class imbalance:

$$FL(p_t) = -\alpha_t (1 - p_t)^7 \log(p_t), \tag{6}$$

where pr – predicted probability for the correct class, γ - focusing parameter (commonly 2), α_e – weighting factor for the class.

Usage Increases focus on hard, misclassified examples like rare hypochromic microcytes.

Balances sensitivity to small and large errors:

$$SmoothL1(x) = \{?(0.5x^2 \,\&"if "|x|<1@|x|-0.5\,\&"otherwise"), \tag{7}$$

where I is the difference between predicted and true bounding box values.

Final output includer Object class label, Bounding box coordinates, Confidence scare, Past-processing uses Non-Maximum Suppression (NMS) to eliminate redundant detections. loU (Intersection ower Union):

$$IoU = \frac{Area\ of\ Overlap}{Area\ of\ Union}, \tag{8}$$

mAPE0.5:

$$mAP60.5 = \frac{1}{N}\sum_{i=1}^{N} AP_i. \tag{9}$$

where AP_1 – average precision for class i, N – total number of classes, mAP@0.5:0.95. Calculated by averaging AP across loU thresholds from 0.5 to 0.95 in steps of 0.05.

The RetinaNet-DDOD model combines deep feature extraction, multi-scale detection, and custom loss functions to achieve high accuracy in detecting small, non-proportional classes such as hypochromic microcytes. Its mathematical design supports robustness and accuracy in medical image analysis.

4 RESULTS

Table 1 compares the YOLOv5, YOLOv7, YOLOv8, Faster RCNN, RetinaNet, and DDOD models on the metrics mAP@0.5 and mAP@0.5:0.95. The DDOD model performed the best.

Table 1. mAP@0.5 and mAP@0.5:0.95 results for different models

Model	Backbone	mAP@0.5 (%)	mAP@0.5:0.95 (%)
YOLOv5	EfficientNet	82.5	65.8
YOLOv7-tiny	E-ELAN	86.2	68.4
YOLOv8	C2f	84.7	67.1
Faster RCNN	ResNet-50	80.3	62.9
RetinaNet	ResNet-50	88.4	70.2
DDOD	ResNet-101	**93.4**	**75.3**

Table 2 shows the mAP@0.5 results for different hyperparameter settings (batch size, learning rate, loss function) of the DDOD model. The best result was obtained with batch size=8, LR=0.001, focal and IoU loss combination.

Table 2. Effect of hyperparameter tuning on DDOD model

Batch Size	Learning Rate (LR)	Function Loss	mAP@0.5 (%)
4	0.01	Focal Loss	90.1
4	0.001	Focal + IoU Loss	91.8
8	0.001	Focal Loss	92.5
8	0.001	Focal + IoU Loss	93.4
16	0.0001	Focal + IoU Loss	92.0

Table 3 compares the AP@0.5 results obtained using 5-fold cross-validation of the DDOD and RetinaNet models. The DDOD model performed 5% better than RetinaNet.

Table 3. 5-Fold Cross-Validation Results (DDOD and RetinaNet)

Model	Fold 1	Fold 2	Fold 3	Fold 4	Fold 5	AP@0.5 (%)
RetinaNet	88.2	89.5	87.8	90.1	88.9	88.9
DDOD	94.5	95.2	93.8	95.0	95.5	**94.8**

The table 4 presents a statistical comparison of the DDOD and RetinaNet models based on the AP@0.5 results. Paired t-test and Cohen's D values confirm the superiority of DDOD.

Table 4. Statistical analysis results (DDOD and RetinaNet)

Model	Average AP@0.5 (%)	Paired t-test (p-qiymat)	Cohen's D
RetinaNet	88.9	0.004	-3
DDOD	94.8	-	-

Table 5 shows the effectiveness of the DDOD model in detecting overlapping cells and reducing false positives, as well as the number of false positives.

Table 5. Detection characteristics and limitations of the DDOD model

Characteristic	Result	Limitation
Detection of overlapping cells	92% accuracy	Small false positive rate
False Positive rate	3.5% (7 errors in 50 images)	Need for more negative samples
Sensitivity to color variations	Moderate sensitivity	Limited by small dataset

Tables 1-5 presents the performance characteristics of the DDOD model in detecting hypochromic microcytes, along with its limitations, based on the experimental results.The study compared the performance of YOLOv5, YOLOv7, YOLOv8, Faster RCNN, RetinaNet and DDOD models. DDOD (ResNet-101) showed the highest results: 93.4% mAP@0.5 and 75.3% mAP@0.5:0.95 (Table 1). Hyperparameter tuning (batch size=8, LR=0.001, focal+IoU loss) increased the performance of DDOD from 90.1% to 93.4% (Table 2). In 5-fold cross-validation, DDOD achieved 94.8% AP@0.5, 5% higher than RetinaNet (Table 3), which was confirmed by statistical analysis (p=0.004, Cohen's D=-3) (Table 4). DDOD detected overlapping cells with 92% accuracy, with a false positive rate of 3.5%, but the small dataset and color sensitivity remained limitations (Table 5). Overall, the DDOD model provided high accuracy and efficiency in diagnosing IDA.

5 CONCLUSION

This study aimed to develop and compare effective object detection algorithms for identifying iron deficiency anemia (IDA) using peripheral blood smear (PBS) images. The initial challenge was the limitations of traditional diagnostic methods, which require experienced specialists, expensive equipment, and are prone to human error. To address these issues, automated systems, specifically deep learning-based object detection models, were proposed. Initially, 386 PBS images were collected from Kasturba Medical College, with 2,550 hypochromic microcytes annotated. The images underwent preprocessing using the Reinhard stain normalization method, which corrected color and illumination variations, thereby enhancing model performance. The study utilized YOLO (v5, v7, v8), Faster RCNN, RetinaNet, and DDOD models. Preliminary results showed that YOLOv7-tiny achieved 86.2% mAP@0.5, a significant improvement over traditional method. However, the RetinaNet-DDOD model (with a ResNet-101 backbone) delivered the highest performance, achieving 93.4% mAP@0.5 and 75.3% mAP@0.5:0.95. Through 5-fold cross-validation, DDOD reached 94.8% AP@0.5, surpassing RetinaNet by 5%, a superiority confirmed by statistical analysis (Paired t-test, p=0.004; Cohen's D=-3). During the study, the DDOD model demonstrated effectiveness in detecting overlapping cells with 92% accuracy and reducing the false positive rate to 3.5%. However, limitations such as a small dataset and sensitivity to color variations were noted. To address these, future plans include adding more images and extending the model to detect other types of anemia. Overall, the study improved diagnostic accuracy from the 80-85% range of traditional methods to 94.8% AP@0.5. This result underscores the importance of automated systems in reducing the workload of hematologists and accelerating the diagnostic process in clinical practice. The study marks a significant step in automating IDA diagnosis, laying a foundation for future expansion.

REFERENCES

[1] *Mclean, E., Cogswell, M., Egli, I., Wojdyla, D., & de Benoist, B.* (2009). Worldwide Prevalence of Anaemia 1993-2005. Geneva: World Health Organization.
[2] *Mohan, H.* (2018). Textbook of Pathology. New Delhi: Jopper Brothers.
[3] *Bruno de Benoist, McLean, E., Egli, I., & Cogswell, M.* (2008). Worldwide Prevalence of Anaemia 1993-2005. Geneva: World Health Organization.
[4] *Pasricha, S. R., Drakesmith, H., Black, J., Hipgrave, D., & Biggs, B. A.* (2021). Iron Deficiency Anemia. Nature Reviews Disease Primers, 7(1), 1-20.

[5] *Wong, A., et al.* (2023). Classification of Abnormal RBCs Using SVM and U-Net. Journal of Medical Imaging, 10(3), 034501.
[6] *Parab, S., et al.* (2022). Customized CNN for RBC Classification. IEEE Transactions on Biomedical Engineering, 69(5), 1456-1465.
[7] *Chandrasiri, S., et al.* (2021). Identification of Anemia Types Using Cell Properties. Medical Physics, 48(9), 5123-5134.
[8] *Pasupa, K., et al.* (2020). CNN-ResNet50 for RBC Classification. Journal of Healthcare Engineering, 2020, 1-12.
[9] *Azam, B., et al.* (2019). Automatic Identification of Microcytic Hypochromic Anaemia. Computers in Biology and Medicine, 112, 103375.
[10] *Rahman, A., et al.* (2022). Central Pallor Based RBC Classification. IEEE Access, 10, 45678-45689.
[11] *Purwar, S., et al.* (2023). Feature Fusion for Hypochromic Microcyte Detection. Biomedical Signal Processing and Control, 80, 104321.
[12] *Nithya, R., & Nirmala, K.* (2022). Detection of Anaemia Using Image Processing Techniques from Microscopy Blood Smear Images. Journal of Physics: Conference Series, 2318, 012043.
[13] *Hortinela, R., et al.* (2021). RBC Identification Using Sobel Operator. IEEE Transactions on Medical Imaging, 40(6), 1678-1689.
[14] *Mundhra, D., et al.* (2022). Localization of Blood Cells Using U-Net. Medical Image Analysis, 75, 102256.
[15] *Naruenatthanaset, K., et al.* (2021). Segmentation of RBCs Using EfficientNet-B1. Journal of Biomedical Informatics, 115, 103698.
[16] *Durant, T., et al.* (2020). Classification of RBCs Using DenseNet. IEEE Journal of Biomedical and Health Informatics, 24(8), 2256-2265.
[17] *Yuningsih, Y., et al*. (2023). Classification of IDA Using CNN. Journal of Clinical Pathology, 76(4), 245-252.
[18] *Wang, C. Y., Bochkovskiy, A., & Liao, H. Y. M.* (2023). YOLOv7: Trainable Bag-of-Freebies Sets New State-of-the-Art for Real-Time Object Detectors. IEEE Conference on Computer Vision and Pattern Recognition (CVPR), 7464-7475.
[19] *Lin, T. Y., et al.* (2017). Focal Loss for Dense Object Detection. IEEE International Conference on Computer Vision (ICCV), 2980-2988.
[20] *Ren, S., He, K., Girshick, R., & Sun, J.* (2015). Faster R-CNN: Towards Real-Time Object Detection with Region Proposal Networks. Advances in Neural Information Processing Systems (NIPS), 91-99.
[21] *Chen, K., et al.* (2019). MMDetection: Open MMLab Detection Toolbox and Benchmark. arXiv preprint arXiv:1906.07155.
[22] *Reinhard, E., Ashikhmin, M., Gooch, B., & Shirley, P.* (2001). Color Transfer Between Images. IEEE Computer Graphics and Applications, 21(5), 34-41.
[23] *Macenko, M., et al.* (2009). A Method for Normalizing Histology Slides for Quantitative Analysis. IEEE International Symposium on Biomedical Imaging (ISBI), 1107-1110.
[24] *Vahadane, A., et al.* (2016). Structure-Preserving Color Normalization and Sparse Stain Separation for Histological Images. IEEE Transactions on Medical Imaging, 35(8), 1962-1971.
[25] Ultralytics. (2023). YOLOv8 Documentation. GitHub Repository. Available at: https://github.com/ultralytics/ultralytics.
[26] *an, M., & Le, Q. V.* (2019). EfficientNet: Rethinking Model Scaling for Convolutional Neural Networks. International Conference on Machine Learning (ICML), 6105-6114.
[27] *He, K., Zhang, X., Ren, S., & Sun, J.* (2016). Deep Residual Learning for Image Recognition. IEEE Conference on Computer Vision and Pattern Recognition (CVPR), 770-778.
[28] *Lin, T. Y., et al.* (2017). Feature Pyramid Networks for Object Detection. IEEE Conference on Computer Vision and Pattern Recognition (CVPR), 2117-2125.
[29] *Zhang, Z., et al.* (2021). Disentangled Dense Object Detection. IEEE Transactions on Pattern Analysis and Machine Intelligence, 44(10), 6452-6465.
[30] *Cohen, J.* (1988). Statistical Power Analysis for the Behavioral Sciences. 2nd ed. Hillsdale, NJ: Routledge.
[31] *Mclean, E., Cogswell, M., Egli, I., Wojdyla, D., & de Benoist, B.* (2009). Worldwide Prevalence of Anaemia 1993-2005. Geneva: World Health Organization.
[32] *Mohan, H.* (2018). Textbook of Pathology. New Delhi: Jopper Brothers.
[33] *Bruno de Benoist, McLean, E., Egli, I., & Cogswell, M.* (2008). Worldwide Prevalence of Anaemia 1993-2005. Geneva: World Health Organization.
[34] *Pasricha, S. R., Drakesmith, H., Black, J., Hipgrave, D., & Biggs, B. A.* (2021). Iron Deficiency Anemia. Nature Reviews Disease Primers, 7(1), 1-20.

[35] *Wong, A., et al.* (2023). Classification of Abnormal RBCs Using SVM and U-Net. Journal of Medical Imaging, 10(3), 034501.
[36] *Parab, S., et al.* (2022). Customized CNN for RBC Classification. IEEE Transactions on Biomedical Engineering, 69(5), 1456-1465.
[37] *Chandrasiri, S., et al.* (2021). Identification of Anemia Types Using Cell Properties. Medical Physics, 48(9), 5123-5134.
[38] *Pasupa, K., et al.* (2020). CNN-ResNet50 for RBC Classification. Journal of Healthcare Engineering, 2020, 1-12.
[39] *Azam, B., et al.* (2019). Automatic Identification of Microcytic Hypochromic Anaemia. Computers in Biology and Medicine, 112, 103375.
[40] *Rahman, A., et al.* (2022). Central Pallor Based RBC Classification. IEEE Access, 10, 45678-45689.

Received: March 25,2025

Citation: *Iskandarova S.N., Tulaganova F.K.* 2025. Efficient model algorithms for processing and recognizing microscopic object of anemia disease. *International Journal of Theoretical and Applied Issues of Digital Technologies*. Volume 8, Issue 2, pp. 95-101. https://doi.org/10.62132/ijdt.v8i2.269.

ЭФФЕКТИВНЫЕ МОДЕЛИ И АЛГОРИТМЫ ОБРАБОТКИ И РАСПОЗНАВАНИЯ МИКРОСКОПИЧЕСКИХ ОБЪЕКТОВ ЗАБОЛЕВАНИЯ АНЕМИЕЙ

[+] *Искандарова С.Н.*[1], *Тулаганова Ф.К.*[1]

[1] Ташкентский университет информационных технологий имени Мухаммада ал-Хоразмий, Ташкент, Узбекистан

[+] sayyora5@mail.ru

Аннотация. Железодефицитная анемия (ЖДА) является распространённой глобальной проблемой здравоохранения, часто диагностируемой на основе анализа мазков периферической крови (МПК), который зависит от квалификации специалистов и дорогостоящего оборудования, что делает его подверженным человеческим ошибкам. Целью данного исследования была разработка и сравнительный анализ алгоритмов обнаружения объектов на основе глубокого обучения для автоматизации диагностики ЖДА с использованием изображений МПК, что позволяет устранить ограничения традиционных методов. Был собран набор данных из 386 изображений МПК в медицинском колледже Кастурба, из которых 249 случаев были подтверждены как ЖДА и 137 — нормальные образцы, с общей аннотацией 2550 гипохромных микроцитов. Изображения были предварительно обработаны методом нормализации окраски Рейнхарда для коррекции вариаций цвета и освещения, что повысило эффективность моделей. В исследовании были протестированы модели YOLO (версий v5, v7, v8), Faster RCNN, RetinaNet и DDOD. Модель YOLOv7-tiny достигла mAP@0.5 в размере 86,2%, превысив показатели традиционных методов (80–85% точности). Однако модель RetinaNet-DDOD с архитектурой ResNet-101 продемонстрировала наилучшие результаты, достигнув mAP@0.5 в 93,4% и mAP@0.5:0.95 в 75,3%. В ходе 5-кратной перекрёстной проверки модель DDOD показала 94,8% AP@0.5, превзойдя RetinaNet на 5%, что подтверждено статистическим анализом (парный t-тест, p=0,004; коэффициент Коэна D=-3). Модель DDOD эффективно выявляла перекрывающиеся клетки с точностью 92% и снизила количество ложноположительных результатов до 3,5%, однако столкнулась с трудностями, обусловленными небольшим объёмом данных и чувствительностью к изменениям цвета. В дальнейшем планируется расширение базы данных и разработка алгоритмов выявления других типов анемии. Настоящее исследование демонстрирует потенциал автоматизированных систем для повышения точности диагностики ЖДА, снижения нагрузки на гематологов и ускорения клинических процессов, создавая основу для более широкого применения в диагностике анемий.

Ключевые слова: Железодефицитная анемия (ЖДА), мазок периферической крови (МПК), обнаружение объектов, глубокое обучение, RetinaNet-DDOD, модели YOLO.